Substrate Sorting by a Supercharged Nanoreactor

Yusuke Azuma, Daniel L. V. Bader, and Donald Hilvert*

Laboratory of Organic Chemistry, ETH Zurich, 8093 Zurich, Switzerland

S *Supporting Information*

ABSTRACT: Compartmentalization of proteases enables spatially and temporally controlled protein degradation in cells. Here we show that an engineered lumazine synthase protein cage, which possesses a negatively supercharged lumen, can exploit electrostatic effects to sort substrates for an encapsulated protease. This proteasome-like nanoreactor preferentially cleaves positively charged polypeptides over both anionic and zwitterionic substrates, inverting the inherent substrate specificity of the guest enzyme approximately 480 fold. Our results suggest that supercharged nanochambers could provide a simple and potentially general means of conferring substrate specificity to diverse encapsulated catalysts.

Protein degradation is a fundamental biological process, essential for maintaining cellular homeostasis, eliminating misfolded or damaged proteins, and generating immunocompetent peptides, among other roles.[1–3] Proteins destined for cleavage often possess specific peptide sequences that are directly recognized by digestive enzymes.[4] Alternatively, they may be equipped with degradation signals that target them to specialized compartments in which the proteases are confined. Such compartments include membrane-bound organelles like the lysosome, which imports tagged substrates via specific uptake pathways,[5,6] or multi-subunit barrel-shaped proteases like the proteasome, which promotes ATP-dependent hydrolysis of ubiquitinated proteins within an enclosed chamber.[7]

Compartmentalization is, in fact, a general strategy for controlling substrate specificity and preventing unwanted off-target reactions. For example, bacteria co-localize sequentially acting enzymes in protein-bound microcompartments to enhance or protect metabolic pathways involved in CO_2 fixation,[8–10] vitamin B_2 synthesis,[11] and degradation of small organic molecules.[9,10] Studies of these structures have highlighted the critical role played by pores in the protective shell for gating small-molecule transport into and out of the compartment.[10] Efforts to utilize protein cages as nanoscale reaction chambers similarly depend on openings in the shell wall for access of substrate molecules. The uptake preferences of a cage can consequently be engineered by altering pore properties. In one instance, negatively charged residues introduced around the pores of bacteriophage MS2 capsids were shown to modulate the activity of an encapsulated phosphatase by limiting transport of negatively charged phosphate ions across the shell wall.[12]

As an alternative to pore engineering, influx into a microcompartment could conceivably be controlled via attractive or repulsive Coulombic interactions between a given substrate and the lumenal surface of a protein cage. We recently designed and evolved a negatively supercharged variant of the cage-forming enzyme *Aquifex aeolicus* lumazine synthase (AaLS-13) that exploits engineered electrostatic interactions to encapsulate positively charged molecules.[13–15] Cryo-electron microscopy studies have revealed that AaLS-13 cages adopt an expanded 360-subunit icosahedral structure with large, keyhole-shaped pores in the cage wall,[16] explaining the rapid and quantitative uptake of cationic cargo like positively supercharged green fluorescent protein, GFP-(+36).[14,17,18] The high affinity of this cationic protein for the lumen of AaLS-13 had made it a practical packaging tag for targeting diverse enzymes to the cage interior.[19–21] Here we exploit this strategy to encapsulate a sequence-specific protease from Tobacco Etch virus (TEV) and show that the resulting proteolytic nanoreactor also sorts potential substrates according to their net charge, promoting uptake and hydrolysis of positively charged peptides and proteins while excluding negatively charged competitors (Figure 1a).
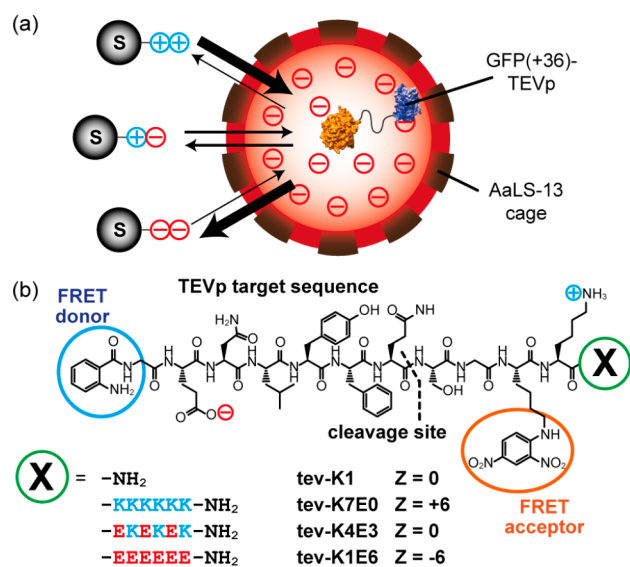

Figure 1. Substrate sorting. (a) Scheme illustrating how electrostatics are exploited to sort substrates for enzymes encapsulated in AaLS-13 protein cages. The tagged substrates are indicated by black spheres (S) with appended positive and/or negative charges. (b) Structures of fluorogenic TEV protease substrates. Z values indicate the theoretical net charge on each peptide at neutral pH.

Our model catalyst was a TEV protease variant possessing the S219V point mutation, which minimizes self-cleavage.[22] This enzyme catalyzes the hydrolysis of a set of fluorogenic substrates derived from the tev-K1 peptide (Figure 1b). These peptides contain the canonical TEV protease recognition site plus an N-terminal aminobenzoic acid (Abz) fluorophore, a dinitrophenol (Dnp) quencher appended to the penultimate lysine, and a C-terminal lysine to increase solubility and neutralize the negatively charged glutamate in the recognition sequence. Separation of the donor and acceptor chromophores upon enzymatic hydrolysis at the TEV cleavage site results in an increase in fluorescence,[23] providing a simple and continuous assay for proteolytic activity. For the substrate sorting experiments, tev-K1 was equipped with charged C-terminal hexapeptide tags consisting of six lysines (tev-K7E0), alternating lysines and glutamates (tev-K4E3), or six glutamates (tev-K1E6). The steady-state kinetic parameters summarized in Table 1 show that all four peptides are cleaved by TEV protease with rates comparable to those for typical TEV substrates (Supporting Information Figure S1a).[22]

Table 1. Kinetic Parameters for Cleavage of Peptide Substrates by Free and Encapsulated TEV Proteases[a,b]

substrate	k_{cat} (s^{-1})	K_M (μM)	k_{cat}/K_M (M^{-1} s^{-1})
	Untagged TEV Protease[c]		
tev-K1	0.16 ± 0.07	24 ± 5	7100 ± 3200
tev-K7E0	0.19 ± 0.06	34 ± 5	5700 ± 2400
tev-K4E3	0.15 ± 0.05	37 ± 9	4400 ± 2500
tev-K1E6	0.13 ± 0.05	21 ± 6	6000 ± 1000
	Free GFP(+36)-TEVp		
tev-K1	0.13 ± 0.01	21 ± 2	6000 ± 100
tev-K7E0	0.14 ± 0.01	28 ± 2	5100 ± 600
tev-K4E3	0.11 ± 0.04	27 ± 7	4100 ± 400
tev-K1E6	0.084 ± 0.019	6.5 ± 1.1	11000 ± 2000[e]
	Encapsulated GFP(+36)-TEVp		
tev-K1	0.064 ± 0.021	63 ± 10	1000 ± 400
tev-K7E0[d]	0.059 ± 0.003	2.1 ± 0.7	28000 ± 2000[e]
tev-K4E3	0.085 ± 0.041	170 ± 80	550 ± 310
tev-K1E6	N.D.[f]	N.D.[f]	130 ± 60

[a]The reactions were monitored at 25 °C and pH 7.4. [b]Data are reported as the mean ± standard deviation (n = 3). [c]The observed steady-state parameters are similar to those reported for cleavage of the TENLYFQSGTRR-NH$_2$ peptide: k_{cat} = 0.19 s^{-1}, K_M = 41 μM, k_{cat}/K_M = 4630 M^{-1} s^{-1}.[22] [d]The reported parameters are derived from the data obtained at low substrate concentrations; the second phase has k_{cat} = 0.13 ± 0.01 s^{-1} and K_M = 24 ± 11 μM. [e]Because of uncertainty in the K_M parameters, these values were determined directly by measuring the reaction rate at 0.5 μM substrate (n = 6). [f]Not determined.

For the encapsulation experiments, S219V TEV protease was fused to the C-terminus of GFP(+36). The resulting construct, GFP(+36)-TEVp, cleaves the tev-K1, tev-K7E0, and tev-K4E3 peptides as efficiently as the untagged enzyme (Table 1 and Figure S1b). In contrast, the anionic tev-K1E6 peptide is processed with a ~2-fold higher k_{cat}/K_M. The latter effect is due entirely to a decrease in the K_M value, consistent with electrostatic attraction of the negatively charged substrate to the enzyme's positively charged GFP(+36) fusion partner.

GFP(+36)-TEVp was encapsulated in AaLS-13 cages by mixing guest and host in different ratios in aqueous buffer, as

previously described for other fusion constructs.[19] The resulting complexes were isolated by size-exclusion chromatography and analyzed by SDS-PAGE and negative stain transmission electron microscopy (TEM). The particles were found to contain both proteins (Figure 2a), with the guest
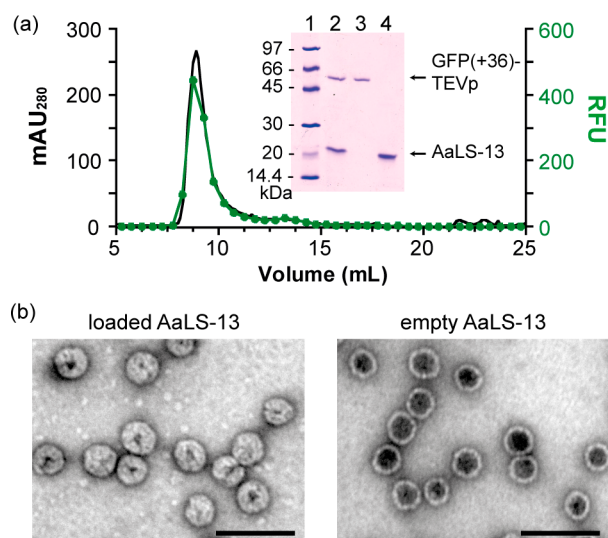

Figure 2. Encapsulation of GFP(+36)-TEVp in AaLS-13. (a) Size-exclusion chromatogram for a mixture of GFP(+36)-TEVp and AaLS-13 (72 guests per cage). Black and green lines respectively indicate 280 nm absorbance and GFP fluorescence for each fraction. The inset shows SDS-PAGE analysis of isolated GFP(+36)-TEVp/AaLS-13 complexes (lane 2), purified GFP(+36)-TEVp (56.7 kDa) (lane 3), and AaLS-13 (17.7 kDa) (lane 4). (b) TEM images of filled and empty AaLS-13 cages. Scale bar = 100 nm.

protease localized in the lumen of the cage (Figure 2b). Loading efficiency, estimated from the 280/488 nm absorbance ratio,[19] was nearly quantitative for mixing ratios up to ~72 enzymes per cage (Figure S2), which corresponds to roughly one GFP(+36) per pentameric capsomer. Attempts to incorporate more than 72 enzymes per cage led to co-precipitation of host and guest.

The catalytic activity of the proteolytic nanoreactors was initially assessed by monitoring the cleavage of the untagged tev-K1 peptide. At 3 μM substrate, a concentration well below the K_M value, the encapsulated protease is ~6-fold less efficient than free enzyme in solution (k_{cat}/K_M = 1000 M^{-1} s^{-1} vs 6000 M^{-1} s^{-1}). At low loading densities (e.g., 4 guests per cage), the encapsulated enzymes retain >90% activity for at least 3 days (Figure S3). At high packing densities (e.g., 72 enzymes per cage), activity drops to 25% of the original value over the same period. The lumenal concentration of enzyme in the latter samples, ca. 8 mM, likely causes aggregation of the poorly soluble TEV protease within the confines of the cage.[24] For this reason, all subsequent kinetic experiments were performed with cage complexes containing 4 enzymes within 36 h after encapsulation. Reducing the number of GFP(+36)-TEVp molecules per AaLS-13 cage has the further benefit of maximizing the lumenal surface area available for interacting with charged substrate molecules. Under the optimized loading conditions, the steady-state k_{cat} and K_M parameters for cleavage of tev-K1 by the GFP(+36)-TEVp/AaLS-13 complex were 0.064 s^{-1} and 63 μM, respectively (Table 1), or 2-fold lower and 3-fold higher, respectively, than the corresponding values for free enzyme.

Encapsulation of GFP(+36)-TEVp in the negatively super-charged AaLS-13 cages substantially alters its substrate specificity (Figure 3, Table 1). As seen for tev-K1, the
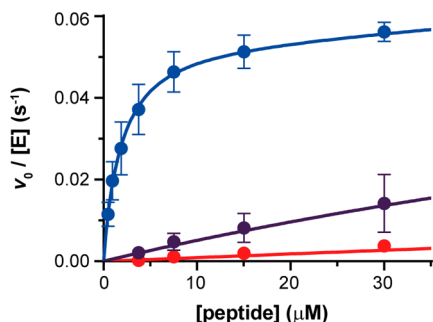

Figure 3. Peptide hydrolysis. Michaelis–Menten plots for the cleavage of tev-K7E0 (blue), tev-K4E3 (purple), and tev-K1E6 (red) catalyzed by encapsulated GFP(+36)-TEVp (40 nM). The reactions were monitored at 25 °C and pH 7.4. The data are reported as the mean ± standard deviation ($n = 3$).

encapsulated enzyme is less active than the free protease with the zwitterionic tev-K4E3 and anionic tev-K1E6 peptides, decreasing the respective k_{cat}/K_M parameter by factors of 7 and 100. In both cases, the decrease is attributable to dramatically increased K_M values, consistent with limited access of these substrates to the negatively charged cage lumen. This effect is particularly pronounced for the negatively charged tev-K1E6 for which saturation was not observed ($K_M > 240~\mu$M).

In contrast to the results with the zwitterionic and anionic substrates, the cationic tev-K7E0 peptide appears to localize in the lumen of the nanoreactor. The kinetics of hydrolysis by the encapsulated GFP(+36)-TEVp shows a biphasic dependence on substrate concentration (Figure 3 blue, Figure S4). Below 15 μM tev-K7E0, comparatively rapid cleavage is observed. The k_{cat}/K_M for this phase is 28 000 M^{-1} s^{-1} (Table 1), which is 5–6 times higher than the k_{cat}/K_M for this substrate with either GFP(+36)-TEVp or the unmodified protease in solution. This increase is achieved by offsetting a 2–3-fold lower k_{cat} by a 14-fold decrease in K_M. Favorable electrostatic interactions between the cationic peptide and the negatively supercharged lumenal surface of the cage would be expected to increase its effective local concentration and thus lower the apparent K_M value.

As the concentration of cationic peptide increases above 15 μM, the initial rates continue to rise but with a shallower dependence on substrate concentration. The steady-state parameters determined for this phase agree well with those determined for the free enzyme in solution. Under these conditions, the cationic substrate, which is present in >1000-fold excess over GFP(+36)-TEVp, presumably displaces the protease from the cage, effectively competing with it for anionic binding sites on the surface of the lumen. In principle, leakage of the protease from the cage could be prevented by covalently linking the enzyme to the lumenal surface, for example, by modifying circularly permuted capsid subunits.[25]

Together, the kinetic data convincingly show that the inherent substrate preferences of GFP(+36)-TEVp are inverted by encapsulation. Thus, when complexed with AaLS-13, GFP(+36)-TEVp cleaves the positively charged tev-K7E0 220-times faster than the negatively charged tev-K1E6, whereas the free enzyme favors tev-K1E6 by a factor of 2.2. To test whether the proteolytic nanoreactor is capable of

selectively processing tagged proteins, we appended a His$_6$ sequence to the N-terminus of GFP via a TEV protease recognition sequence (Figure 4a). Two new GFP variants,
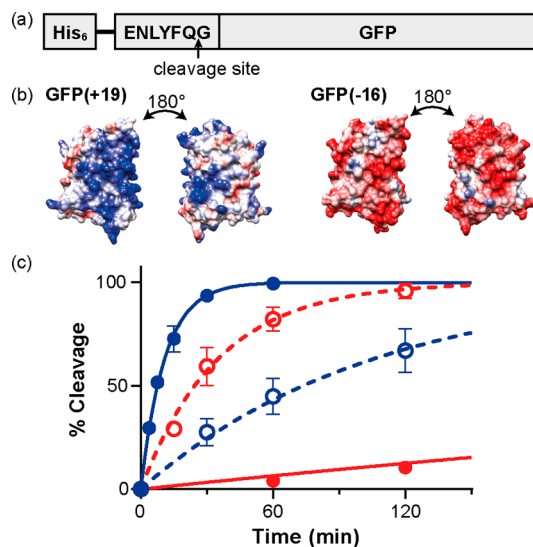

Figure 4. Protein hydrolysis. (a) A GFP construct containing an N-terminal His$_6$ tag and a TEVp cleavage site. (b) Surface charge of GFP(+19) (left) and GFP(−16) (right); thresholds ±15 $k_B T/e$. The models were constructed using the crystal structure of superfolder GFP (PDB ID: 2B3P). (c) Cleavage of H$_6$-TEV-GFP(+19) (blue) or H$_6$-TEV-GFP(−16) (red) catalyzed by GFP(+36)-TEVp free in solution (open circles and dashed lines) or encapsulated in AaLS-13 cages (filled circles and solid lines). The reactions were performed at room temperature at pH 7.4. The data are reported as the mean ± standard deviation ($n = 3$). As a first approximation, the data were fit to the equation for a single exponential curve.

containing clusters of either positive or negative residues, were constructed for this purpose (Figure 4b). The resulting proteins, H$_6$-TEV-GFP(+19) and H$_6$-TEV-GFP(−16), have identical scaffolds but distinct isoelectric points (pI) of 9.8 and 5.2 (Table S1), reflecting their different net surface charge.

GFP(+36)-TEVp-catalyzed hydrolysis of the H$_6$-TEV-GFP substrates was monitored by SDS-PAGE. As was the case for the tagged tev-K1 peptides, free enzyme preferentially cleaves the negatively charged protein: in the presence of 200 nM protease, the half-lives ($\tau_{1/2}$) for cleavage of 10 μM H$_6$-TEV-GFP(+19) and H$_6$-TEV-GFP(−16) were 65 and 25 min, respectively (Figure 4C, Figure S5, and Table S2). This modest 2.6-fold specificity, which reflects favorable electrostatic interactions between the negatively charged substrate and positively charged catalyst, was inverted upon encapsulation of the protease in AaLS-13 cages (Figure 4C, Figure S5, and Table S2). The encapsulated enzyme cleaves H$_6$-TEV-GFP(+19) ($\tau_{1/2} = 7.6$ min) 93 times faster than GFP(−16) ($\tau_{1/2} = 710$ min). As for the short peptides, enhanced cleavage of the positively charged protein and reduced hydrolysis of its negatively charged counterpart are both consistent with a simple electrostatic model in which the negatively super-charged nanoreactor either concentrates or excludes the corresponding substrate.

The protease/cage complex described in this report functions much like an artificial proteasome. Rather than recognizing a ubiquitin tag, however, it exploits engineered electrostatic interactions to promote preferential uptake and hydrolysis of positively charged peptides and proteins and to

discriminate against zwitterionic or negatively charged molecules. This proteasome mimic has a number of advantages over previously described synthetic polymers that also exploit electrostatic interactions to modulate protease activity.[26,27] First, it is completely modular and forms spontaneously under a wide range of conditions, including at physiological ionic strength, simply by mixing the components either in vitro or in vivo.[13,18] Second, as a genetically programmable material, its properties can be precisely tailored by standard molecular biological approaches.

Artificially compartmentalized proteases could be useful to remove and/or reveal peptide tags that direct subcellular localization of proteins,[28,29] control cytosolic protein concentrations for directed evolution,[30,31] or, in combination with a sequentially acting enzyme, conditionally activate/destroy peptide hormones or other substrates.[32,33] Because compartmentalization provides a simple means of tuning the environment around an enzyme, allowing only appropriately tagged substrates access, it is likely that these supercharged nanochambers can be adapted to modulate the properties of many other catalytic processes.

■ ASSOCIATED CONTENT

Ⓢ Supporting Information

The Supporting Information is available free of charge on the ACS Publications website at DOI: 10.1021/jacs.7b11210.

> Experimental procedures, Michaelis−Menten plots, size-exclusion chromatograms, TEM images, kinetic parameters, and SDS-PAGE, including Figures S1−S8 and Tables S1−S5 (PDF)

■ AUTHOR INFORMATION

Corresponding Author
*hilvert@org.chem.ethz.ch

ORCID Ⓞ
Yusuke Azuma: 0000-0003-3543-3159
Donald Hilvert: 0000-0002-3941-621X

Notes
The authors declare no competing financial interest.

■ ACKNOWLEDGMENTS

■ REFERENCES

(1) Baumeister, W.; Walz, J.; Zühl, F.; Seemüller, E. Cell 1998, 92, 367−380.
(2) Goldberg, A. L. Biochem. Soc. Trans. 2007, 35, 12−17.
(3) Ciechanover, A. Cell Death Differ. 2005, 12, 1178−1190.
(4) Pogson, M.; Georgiou, G.; Iverson, B. L. Curr. Opin. Biotechnol. 2009, 20, 390−397.
(5) Dice, J. F. Trends Biochem. Sci. 1990, 15, 305−309.
(6) Kaushik, S.; Cuervo, A. M. Trends Cell Biol. 2012, 22, 407−417.
(7) Ciechanover, A. Cell 1994, 79, 13−21.
(8) Codd, G. A.; Marsden, W. J. N. Biol. Rev. 1984, 59, 389−422.
(9) Yeates, T. O.; Kerfeld, C. A.; Heinhorst, S.; Cannon, G. C.; Shively, J. M. Nat. Rev. Microbiol. 2008, 6, 681−691.
(10) Kerfeld, C. A.; Heinhorst, S.; Cannon, G. C. Annu. Rev. Microbiol. 2010, 64, 391−408.
(11) Ladenstein, R.; Fischer, M.; Bacher, A. FEBS J. 2013, 280, 2537−2563.
(12) Glasgow, J. E.; Asensio, M. A.; Jakobson, C. M.; Francis, M. B.; Tullman-Ercek, D. ACS Synth. Biol. 2015, 4, 1011−1019.
(13) Wörsdörfer, B.; Woycechowsky, K. J.; Hilvert, D. Science 2011, 331, 589−592.
(14) Wörsdörfer, B.; Pianowski, Z.; Hilvert, D. J. Am. Chem. Soc. 2012, 134, 909−911.
(15) Beck, T.; Tetter, S.; Künzle, M.; Hilvert, D. Angew. Chem., Int. Ed. 2015, 54, 937−940.
(16) Sasaki, E.; Böhringer, D.; van de Waterbeemd, M.; Leibundgut, M.; Zschoche, R.; Heck, A. J. R.; Ban, N.; Hilvert, D. Nat. Commun. 2017, 8, 14663.
(17) Lawrence, M. S.; Phillips, K. J.; Liu, D. R. J. Am. Chem. Soc. 2007, 129, 10110−10112.
(18) Zschoche, R.; Hilvert, D. J. Am. Chem. Soc. 2015, 137, 16121−16132.
(19) Azuma, Y.; Zschoche, R.; Tinzl, M.; Hilvert, D. Angew. Chem., Int. Ed. 2016, 55, 1531−1534.
(20) Frey, R.; Mantri, S.; Rocca, M.; Hilvert, D. J. Am. Chem. Soc. 2016, 138, 10072−10075.
(21) Frey, R.; Hayashi, T.; Hilvert, D. Chem. Commun. 2016, 52, 10423−10426.
(22) Kapust, R. B.; Tözsér, J.; Fox, J. D.; Anderson, D. E.; Cherry, S.; Copeland, T. D.; Waugh, D. S. Protein Eng., Des. Sel. 2001, 14, 993−1000.
(23) Carmona, A. K.; Schwager, S. L.; Juliano, M. A.; Juliano, L.; Sturrock, E. D. Nat. Protoc. 2006, 1, 1971−1976.
(24) Cabrita, L. D.; Gilis, D.; Robertson, A. L.; Dehouck, Y.; Rooman, M.; Bottomley, S. P. Protein Sci. 2007, 16, 2360−2367.
(25) Azuma, Y.; Herger, M.; Hilvert, D. J. Am. Chem. Soc. 2017, DOI: 10.1021/jacs.7b10513.
(26) Roy, R.; Sandanaraj, B. S.; Klaikherd, A.; Thayumanavan, S. Langmuir 2006, 22, 7695−7700.
(27) Kurinomaru, T.; Tomita, S.; Hagihara, Y.; Shiraki, K. Langmuir 2014, 30, 3826−3831.
(28) von Heijne, G. eLS [Online]; John Wiley & Sons Ltd: Chichester, UK, 2005; http://onlinelibrary.wiley.com/doi/10.1038/npg.els.0005050/full (accessed Dec 5, 2017).
(29) van Tetering, G.; Vooijs, M. Curr. Mol. Med. 2011, 11, 255−269.
(30) Neuenschwander, M.; Butz, M.; Heintz, C.; Kast, P.; Hilvert, D. Nat. Biotechnol. 2007, 25, 1145−1147.
(31) Butz, M.; Neuenschwander, M.; Kast, P.; Hilvert, D. Biochemistry 2011, 50, 8594−8602.
(32) LeMosy, E. K.; Hong, C. C.; Hashimoto, C. Trends Cell Biol. 1999, 9, 102−107.
(33) Cerenius, L.; Kawabata, S.; Lee, B. L.; Nonaka, M.; Söderhäll, K. Trends Biochem. Sci. 2010, 35, 575−583.